Available online at www.sciencedirect.com
ScienceDirect
Journal of Hazardous Materials 152 (2008) 640–647
Journal of Hazardous Materials
www.elsevier.com/locate/jhazmat

Preparation and characterization of sodium iron titanate ion exchanger and its application in heavy metal removal from waste waters

Marceline N. Akieh [a], Manu Lahtinen [b], Ari Väisänen [b], Mika Sillanpää [a,*]

[a] *Laboratory of Applied Environmental Chemistry, Department of Environmental Sciences, University of Kuopio, Patteristonkatu 1, FIN-50100 Mikkeli, Finland*
[b] *Department of Chemistry, University of Jyväskylä, P.O. Box 35, FIN-40014 JY, Finland*

Received 28 December 2006; received in revised form 26 June 2007; accepted 10 July 2007
Available online 20 July 2007

Abstract

The ion exchange properties of sodium iron titanates, namely, $NaFeTiO_4$, $Na_2Fe_2Ti_6O_{16}$ and iron-doped sodium nonatitanate were investigated. Conventional solid state and sol–gel methods were used in the synthesis of the sodium iron titanates. Structural characterization of the materials was performed with powder X-ray diffraction (XRD), thermogravimetry (TG), scanning electron microscopy (SEM) equipped with energy dispersive spectrometer (EDS) and with inductively coupled plasma optical emission spectrometry (ICP-OES). Based on TG analyses, the novel iron-doped sodium nonatitanate was proven to be a member of the layered titanate family. The different sodium iron titanates were compared based on the efficiency in separating Ni from aqueous streams by conducting batch experiments with a batch factor of 1000 ml/g. Iron-doped sodium nonatitanate exhibited the best ion exchange performance compared to the other sodium iron titanates studied. It was found to be selective for nickel over potassium and showed 99% removal efficiency for Ni.

Keywords: Sodium iron titanate; Iron-doped sodium nonatitanate; Ion exchange; Heavy metal; Waste water

1. Introduction

Environmental legislation on waste water containing heavy metal disposal is becoming more stringent. Heavy metal pollution of water and soil is known to affect the ecology adversely, thereby, causing health hazards in humans. Major contributors to environmental pollution with toxic metals are released from anthropogenic sources such as metallurgical, galvanizing, metal finishing, electroplating, mining, power regeneration, electronic device manufacturing and tannery industries [1].

A number of treatment methods have been utilized in removing metals from industrial waste waters. The most commonly applied methods are: precipitation, ion exchange, solvent extraction, evaporation, electrodialysis and reverse osmosis. Amongst these methods evaporation, reverse osmosis and electrodialysis exhibit no selectivity whereas precipitation, solvent extraction and ion exchange are selective for specific ions of interest. A major disadvantage of precipitation is the huge generation of sludge that needs extra disposal. Solvent extraction also involves the use of extraction chemicals that are often toxic organic substances. Ion exchange has several benefits compared to other methods because it is relatively clean and energy efficient method, which also features selectivity for certain ions even in solutions of low concentration of the target ion. Furthermore, it has high treatment capacity, high removal efficiency, fast kinetics [1–3] and can also be utilized in metal recovery and water reuse, which are of economical importance [4].

Both organic and inorganic ion exchangers have been synthesized and exploited in heavy metal removal from waste effluents. During the last few decades inorganic ion exchangers have become increasingly popular because of certain advantages over organic resins such as resistance towards high ionizing radiation, stability at higher temperatures and selectivity towards certain metal ions [5]. Within the last few years various types of inorganic ion exchangers such as titanate [6–11], molybdate [12–15], zirconia [16], phosphate [17], tungstate [18],

* Corresponding author. Tel.: +358 400205215; fax: +358 15 3556363.
E-mail address: mika.sillanpaa@uku.fi (M. Sillanpää).

0304-3894/$ – see front matter © 2007 Elsevier B.V. All rights reserved.
doi:10.1016/j.jhazmat.2007.07.049

Nomenclature

a, b	Langmuir parameters
BF	batch factor
C_e	concentration at equilibrium
C_i	initial concentration
K, n	Freundlich parameters
K_d	distribution coefficient
pH_e	pH at equilibrium
Q_e	amount of metal (Ni) adsorbed at equilibrium

silicate [19–22], hydrous metal oxides [23–25] and silicoantimonate [26] have been synthesized and investigated as potential materials for the removal of heavy metal ions. However, new innovations and ion exchange materials are constantly sought due to diverse nature of the waste water media.

Sodium iron titanate is another type of inorganic ion exchanger with only a limited number of similar related studies found in the literature. The basic structural unit that builds up the entire framework of sodium iron titanates is the (Ti, Fe)O_6 octahedron. The octahedral units share edges at one level that combine with similar units to form strings of octahedra. These chains are either combined to form layers or tunnel type titanates. Exchangeable alkaline metal, e.g. sodium, is located between the interlayers or within the tunnels to maintain charge balance [27,28].

The aim of conducting this study is to investigate the efficiency of a novel iron-doped sodium nonatitanate with regard to nickel removal from waste water. Also, the ion exchange properties of iron-doped sodium nonatitanate are compared to other existing sodium iron titanates such as $NaFeTiO_4$ and $Na_2Fe_2Ti_6O_{16}$.

2. Materials and methods

2.1. Chemicals

Unless otherwise stated, all reagents used were of analytical grade and purchased from Merck. TiO_2 was purchased from Alfa Aesar GmbH & Co. KG, NaOH from J.T. Baker. $FeCl_3{\cdot}6H_2O$, NHO_3 (65%, p.a.), and HCl (36–38%, p.a.) were supplied by Riedel-de-Haën. High purity water (18 MΩ cm, ELGA Maxima, Elga Ltd., Bucks, GB) was used in preparing solutions unless otherwise stated. Reagents were used as received without further purification. The standard stock solutions (1000 mg/l) for the ICP-OES and F-AAS measurements were supplied by Merck.

2.2. Equipments

2.2.1. Atomic absorption spectrometry

Perkin-Elmer 460 air-acetylene flame atomic absorption spectrometer (F-AAS) at 341.5 nm wavelength was use to determine the concentration of nickel in solution before and after equilibrium.

2.2.2. X-ray powder diffractometry

The X-ray powder diffraction data were obtained at room temperature by the Huber imaging-plate Guinier camera 670 using germanium monochromated Cu $K\alpha_1$ radiation ($\lambda = 1.5406$ Å; 45 kV, 25 mA). The measurements were carried out in Guinier-type transmission geometry with the angle of incidence 45° to the sample normal. The hand-ground samples were prepared on the paraffin-coated Mylar foil of 3.5 μm thickness, which was mounted on vertical sample holder oscillating horizontally. The X-ray diffraction data were collected with a position sensitive imaging-plate detector using 2θ-angle range of 4–100°. The collected data were acquired from the detector by steps-scanning laser with a step resolution of 0.005° 2θ generating dataset with 19,200 data points. A receiving slit of 4 mm was used in front of the detector window to diminish the extent of asymmetry of the peak profiles occurring especially on low 2θ-range.

The qualitative and semi-quantitative search/match analyses were made by the Bede ZDS Search/Match Software for Windows® [29] with embedded ICDD Powder Diffraction PDF2 Database [30].

2.2.3. Scanning electron microscopy

Morphology and elemental analysis of the iron-doped sodium nonatitanate were performed with a Hitachi S-4800 SEM equipped with EDS. The sample was placed on a carbon tape with silicon adhesive and was mounted on an aluminum stub. The instrument was operated at 5–10 kV and 30,000× magnification.

2.2.4. ICP-OES spectrometry

The measurements of the concentrations of Ti, Fe and Na of the iron-doped sodium nonatitanate were performed with a Perkin-Elmer (Norwalk, CT, USA) model Optima 4300 DV inductively coupled plasma optical emission spectrometry. The determination of element concentrations was performed with default parameters of the instrument (nebulizer flow 0.8 l/min, auxiliary gas flow 0.2 l/min, plasma gas flow 15 l/min and plasma power of 1400 W). Two wavelengths for each of the investigated element were tested by radially viewed plasma. The appropriate wavelengths used in the final determination were 336.121, 238.204 and 589.592 nm for Ti, Fe and Na, respectively. All the concentration measurements were carried out using a four-point calibration. Multi-element calibration standards were used for all elements.

2.2.4.1. Ultrasound-assisted digestion procedure. A sample of about 20 mg of the iron-doped sodium nonatitanate was accurately weighed into a 50 μl aluminum pan. The sample was transferred into a 15 ml polyethylene centrifuge tube into which 1 ml of *aqua regia* and 1 ml of HF (40%, p.a.) was added. The centrifuge tube was closed and placed into a 650 W, 35 kHz, Model Transsonic 820/H ultrasonic water bath (ELMA, Singen, Germany). The sonication procedure was carried out at a temperature of about 50 °C. The sonication procedure was divided into 3-min steps with the sample bottle shaken by hand between each step. The shaking was used to prevent sedimentation. After

12 min sonication the total dissolution of sample was obtained. After digestion the sample solution was transferred into a 100 ml volumetric polyethylene flask and diluted to volume with water.

2.2.5. Thermogravimetry measurements

The thermal behavior of the compounds was examined with Perkin-Elmer PYRIS DIAMOND TG/DTA thermogravimetric analyzer. The measurements were carried out in platinum pans under air atmosphere (a flow rate of 150 ml/min) with a heating rate of 10 °C/min at a temperature range of 28–1000 °C. The temperature calibration of the TG/DTA equipment was made using the melting points of five reference materials (In, Sn, Zn, Al, and Au). The weight balance was calibrated by measuring a standard weight as a function of temperature. The sample weights used in the measurements were 9–15 mg.

2.3. Synthesis

Sodium iron titanates of this nature $NaFeTiO_4$ and $Na_2Fe_2Ti_6O_{16}$ were synthesized by conventional solid-state route. $NaFeTiO_4$ was synthesized as follows: 1.03 g of Na_2CO_3, 0.77 g of Fe_2O_3 and 1.55 g of TiO_2 were mixed thoroughly in a mortar with a few drops of acetone to ease the mixing. The mixing time was 15–20 min to ensure complete evaporation of acetone. The mixture was transferred to a platinum crucible and heated at 900 °C with a slow injection of air for 24 h. It was then re-ground and heated again at the same temperature and time. The synthesis of $Na_2Fe_2Ti_6O_{16}$ followed a similar procedure except that quantities of the reagents were as follows: 0.58 g of Na_2CO_3, 0.44 g of Fe_2O_3 and 2.18 g of TiO_2.

Clearfield and Lehto [31] reported that titanates of the highest series (e.g. sodium nonatitanates) have been obtained only by synthetic routes other than conventional solid state. Therefore, the novel iron-doped sodium nonatitanate ($Na_4Fe_xTi_{9-x}O_{20}\cdot nH_2O$) was synthesized by the sol–gel method. The amorphous end product was afterwards hydrothermally treated to increase crystallinity. In the synthesis of iron-doped sodium nonatitanate; 10 ml of methanol was added to 10 ml of titanium isopropoxide (TIP). 2.704 g of NaOH was dissolved in 100 ml of water. The NaOH solution was added into the methanol/TIP mixture. The mixture was subjected to stirring to disperse clumpy precipitate, thereafter 10 ml of 10% $FeCl_3\cdot 6H_2O$ solution was added. Finally, 100 ml of excess water was added for a faster hydrolysis and condensation reaction to occur [32]. The gel was stirred continuously for 1 h to complete the reaction. The volume was reduced by heating and then transferred to a 100 ml Teflon cup. The Teflon cup was fitted in a Parr autoclave and subjected to 153 °C internal temperature and pressure of 2 bars for 2 days. After hydrothermal treatment, the substance was filtered, flushed with excess distilled water to washout excess NaOH and dried at 100 °C.

2.4. Ion exchange studies

The ion exchange properties of the synthesized sodium iron titanates were investigated in terms of selectivity for nickel in potassium solutions, effect of initial concentration, time to attain equilibrium and effect of pH. All ion exchange experiments were performed in the batch mode with a batch factor of 1000 ml/g and subdued to unidirectional shaking on a reciprocal shaker at room temperature.

2.4.1. Equilibrium studies

In the equilibrium studies, 10 mg of ion exchanger was shaken in 10 ml of 100 mg/l Ni solution. Ni solution was prepared by dissolving the appropriate amount of $Ni(NO_3)_2\cdot 6H_2O$ salt in water. The experiment was performed at different time intervals, i.e. from 5 min to 2 days. After the specified times the ion exchanger was separated from the liquid phase by centrifugation ($4000 \times g$) for 10 min. The pH and remaining nickel concentration of the supernatant was analyzed with InoLab pH 730 meter and F-AAS, respectively.

To determine the time to reach equilibrium, percent sorption was plotted against time. The percent sorption was calculated according to Eq. (1) below.

$$\text{Sorption}\,(\%) = \frac{C_\text{i} - C_\text{e}}{C_\text{i}}\,100 \tag{1}$$

where C_i is the initial metal concentration (mg/l) and C_e is the concentration of metals remaining in solution at equilibrium (mg/l).

2.4.2. Adsorption isotherm and the effect of initial concentration on adsorption

A stock solution of 1000 mg/l Ni was prepared by dissolving 0.4955 g of $Ni(NO_3)_2\cdot 6H_2O$ in 100 ml of water. Six concentrations (10–200 mg/l) used in the experiment were made by diluting this stock solution. Ten milligram of sodium iron titanates was equilibrated (on a shaker) in 10 ml of the various nickel solutions for 24 h. The experiments were performed at solution pH of 4.86–5.47. The equilibrium pH and equilibrium concentration was determined by the InoLab pH meter and F-AAS, respectively.

To establish the adsorption isotherms, the adsorption data is fitted to the linearized Langmuir (Eq. (2)) and Freundlich (Eq. (3)) equations.

$$\frac{C_\text{e}}{Q_\text{e}} = \frac{1}{ab} + \frac{C_\text{e}}{a} \tag{2}$$

$$\log Q_\text{e} = \log K + \frac{1}{n\log C_\text{e}} \tag{3}$$

where Q_e is the amount of metal adsorbed at equilibrium, calculated as $(C_i - C_\text{e}) \times v/m$ (mg/g), C_i and C_e the respective initial and equilibrium Ni concentration (mg/l), v/m the ratio of the volume of solution (l) to the mass of dry exchanger (g), a and b the Langmuir parameters signifying the adsorption capacity and energy of adsorption, respectively, while K and n are the Freundlich parameters signifying the adsorption capacity and adsorption isotherms.

2.4.3. Effect of pH

Ten milligram of each exchanger was shaken in 10 ml of 10 mg/l Ni solution at a pH range of 2–8. The pH of the solution

was adjusted with 0.05 M HCl and 0.05 M NaOH until equilibrium was reached. Nickel concentration at equilibrium was determined as mentioned before.

2.4.4. Selectivity of nickel in potassium solutions

$Ni(NO_3)_2{\cdot}6\ H_2O$ was dissolved in K solutions of varying concentrations (200–1500 mg/l). The concentration of Ni was 100 mg/l in each case. Ten milligram of exchanger was equilibrated in 10 ml of K/Ni solution for 24 h. Nickel concentration at equilibrium was determined as described before. Based on preliminary experiments with Ni in K-based buffer solutions, a marked difference in the uptake behavior of the sodium iron titanates was observed, thus further experiments were performed in K solution as a medium.

The selectivity of the ion exchangers for Ni over K was evaluated on the basis of their distribution coefficients (K_d). K_d indicates the processing ion exchange capacity and the selectivity of an ion exchanger under specified conditions for cations especially found in trace amounts [33,34]. K_d is the distribution of ions between the ion exchanger and the external solution and was calculated as in Eq. (4).

$$K_d = \frac{C_i - C_e}{C_e}\,BF \tag{4}$$

where C_i and C_e are the initial and equilibrium concentrations, respectively (mg/l) and BF is the batch factor (ml/g).

3. Results and discussion

For simplicity, the sodium iron titanates are assigned as $SFeTi_9$ ($Na_4Fe_xTi_{9-x}O_{20}{\cdot}nH_2O$), CFeTi ($NaFeTiO_4$) and CFe_2Ti_6 ($Na_2Fe_2Ti_6O_{16}$), where S and C indicate the method of preparation, i.e. sol–gel and conventional solid-state synthesis, respectively.

3.1. Structural characterization

XRD patterns of the compounds that were synthesized by conventional solid state showed phase mixtures, in which the main component of the mixture was identified as the desired product. The minor components were identified as different types of sodium titanates (typically $NaTi_2O_4$, $Na_2Ti_3O_7$ and $Na_2Ti_6O_{13}$). In addition, some trace amounts of non-stoichiometric sodium iron titanates and iron oxide were also found. The main phases of sample CFeTi is $NaFeTiO_4$ with close to equal proportion of $Na_{2.08}Ti_4O_9$ and were identified in comparison with PDF2 entries 73–424 and 84–2047, respectively. The minor phases in this sample were identified as $Na_{0.75}Fe_{0.75}Ti_{0.25}O_2$ (74–1547) and cubic Fe_2O_3 (39–238). The CFe_2Ti_6 consisted of a main phase that is $Na_2Fe_2Ti_6O_{16}$ (70–637) and from smaller fraction of sodium tri- and hexatitanates, having also trace amounts of $Na_{0.6}Fe_{0.8}Ti_{1.2}O_4$ (87–551) and cubic Fe_2O_3. From the XRD data obtained at room temperature for $SFeTi_9$, only weak (broad) diffraction peaks corresponding to poorly crystalline sodium (iron) nonatitanate phase without the presence of other phases was observed (Fig. 1, lower). Since only some of the Ti sites in the unit cell of the layered sodium nonatitanate are replaced randomly by the Fe atoms and, thus, the layered structure model is still preserved, it was expected that the diffraction patterns of both non-doped and iron-doped sodium nonatinates would be rather identical. It is also noted that the diffraction peak positions of sodium nonatitanates with different water contents shift as the d-spacing of diffracting titanate layers changes with varying water content [31]. The tentative indication of the presence of iron in the sample can also be deduced from XRD data of the TG residue of sample $SFeTi_9$ (Fig. 1, upper) that revealed the main three decomposition to be sodium iron titanate ($Na_2Fe_2Ti_6O_{16}$) and sodium hexa- and trititanates ($Na_2Ti_6O_{13}$, $Na_2Ti_3O_7$). Additional measurements (ICP-OES and SEM + EDS) were performed to further characterize the formation of the iron-doped sodium nonatitanate.

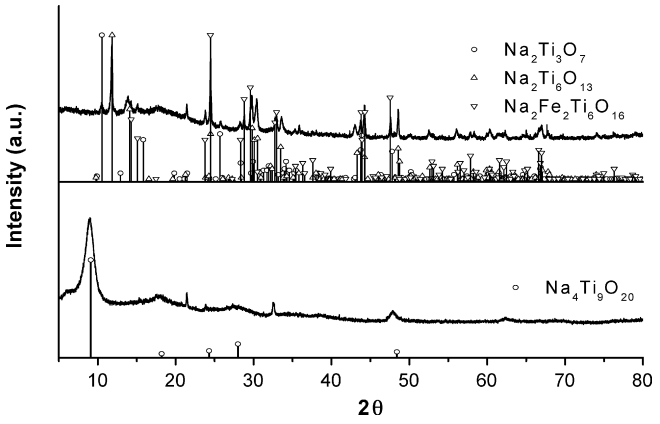

Fig. 1. X-ray diffraction patterns of $SFeTi_9$: measured from fresh sample at room temperature (lower) and from TG residue of the sample at 1000 °C (upper).

Fig. 2 presents the EDS spectra obtained from $SFeTi_9$. All the elements that are present in the iron-doped sodium nonatitanate are shown. The elemental composition by weight percent and atomic percent is presented in Table 1. According to these results approximately 7% by weight of iron is present in the compound taking into consideration that there was the presence of trace

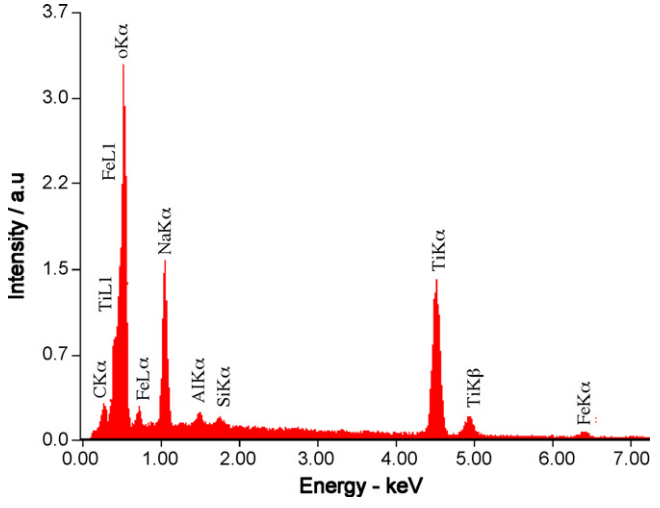

Fig. 2. EDS spectra of iron-doped sodium nonatitanate.

Table 1
Quantification of iron-doped sodium nonatitanate based on EDAX ZAF standardless method after removing the influence from the background carbon

Element	Weight (%)	Atomic (%)
O	36.45	59.71
Na	9.52	10.85
Al	0.64	0.62
Si	0.5	0.47
Ti	45.31	24.79
Fe	7.58	3.56

amounts of other elements (Si and Al) and also that hydrogen was not measured by the instrument. The instrument can measure only elements above carbon. The presence of C, Si and Al is explained to rise from the tape and stub on which the sample was mounted during the SEM measurements. Carbon peak may also arise from the carbonizing electron beam used during the SEM measurements. Fig. 3 presents the SEM micrograph of iron-doped sodium nonatitanate. The image revealed smaller particles that are needle shaped in the size range of 1–3 μm by 40–80 nm. The smaller particles are clustered together forming larger particles of several μm in size.

Elemental content of $SFeTi_9$ was quantified also by ICP-OES technique, which revealed iron, titanium and sodium contents of 47 ± 5, 360 ± 40 and 73 ± 8 mg/g (mean ± standard deviation of three replicate samples), respectively. By combining the information obtained from the ICP-OES and TG and SEM measurements, the molar Fe ratio in the iron-doped sodium nonatitanate is deduced to be $x = \sim 0.8$ ($Na_4Fe_xTi_{9-x}O_{20}\cdot nH_2O$) when the observed weight loss in the TG curve is estimated to represent eight moles of water. To check the validity of the procedure, similar quantification was also made with non-doped sodium nonatinate sample and expected molar ratios were found for both titanium and sodium.

From the TG analysis of the ion exchangers, weight loss of 14.8% was observed for $SFeTi_9$ at temperature range of 30–346 °C (Fig. 4), which is caused by release of water located between (Ti, Fe)O_6 octahedral layers [31,35]. Negligible weight loss was observed in the TG curves from 25 to 1000 °C for CFeTi and CFe_2Ti_6 samples.

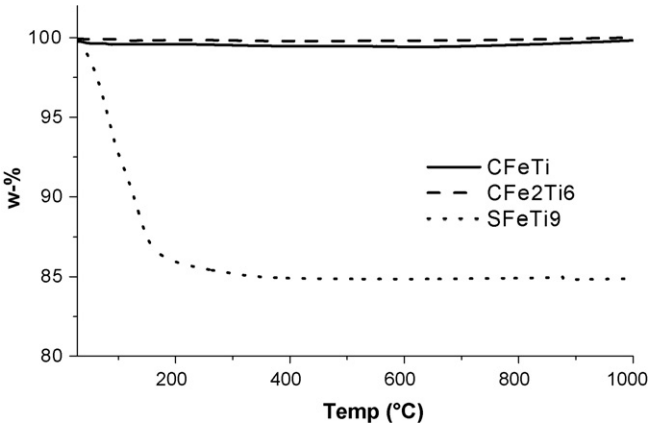

Fig. 4. TG curves of sodium iron titanates obtained at the temperature range of 28–1000 °C showing constancy in CFeTi and CFe_2Ti_6 and 14.8% weight lost at 30–346 °C for $SFeTi_9$.

3.2. Ion exchange studies

As seen from Fig. 5, the rate of Ni exchange by the sodium iron titanates varied, as the kinetics is faster for $SFeTi_9$ than for CFeTi and CFe_2Ti_6. The adsorption percentage increases with time until equilibrium is attained. At equilibrium, the maximum adsorption of Ni by $SFeTi_9$ is 99.9%, while for CFe_2Ti_6 and CFeTi it is only 37 and 17%, respectively. Equilibrium is attained within 3 h for $SFeTi_9$ while for CFeTi and CFe_2Ti_6 it is attained within 24 h. Therefore, a contact time of 24 h was selected for the subsequent experiments.

The effect of concentration on adsorption of Ni by the sodium iron titanates was investigated at initial Ni concentrations of 10–200 mg/l at pH 4.86–5.47. The percent sorption was calculated as in Eq. (1) and plotted against initial concentration (Fig. 6). It was found that percent adsorption remains constant at lower initial concentrations and decreases at higher initial concentrations for $SFeTi_9$ and CFe_2Ti_6. CFeTi, on the other hand,

Fig. 3. SEM image of iron-doped sodium nonatitnate.

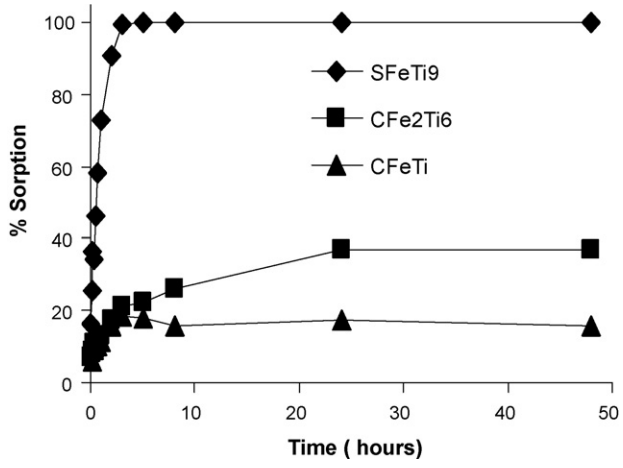

Fig. 5. % Sorption against time to establish equilibrium for the exchange of Ni by sodium iron titanates at initial pH of 5.47.

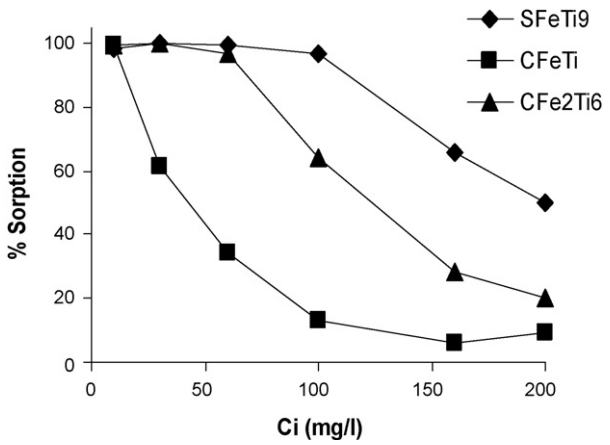

Fig. 6. The effect of initial concentration on the removal of Ni by sodium iron titanates at solution pH of 4.86–5.47.

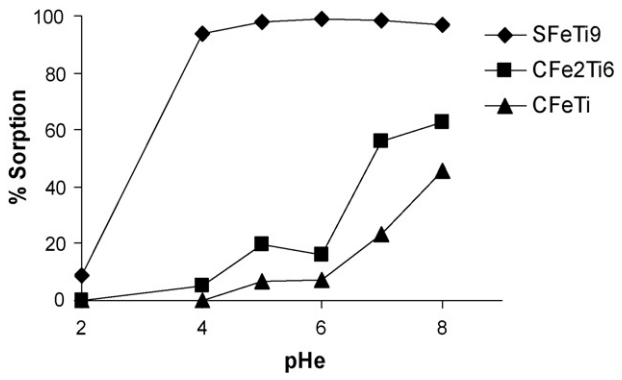

Fig. 7. A plot of % sorption as a function of equilibrium pH (pH_e) to investigate the effect of pH on adsorption of Ni by sodium iron titanates at initial Ni concentration of 10 mg/l.

showed a decrease of adsorption percentage with increasing initial concentration. It was also observed that $SFeTi_9$ exhibits an overall good performance in the separation of Ni at the initial concentrations studied.

The initial pH before the start of the experiment and the equilibrium pH (i.e. pH after 24 h of contact time) were measured at the different initial concentrations (Table 2). It is noteworthy to mention that in this particular set of experiments the pH of the systems was not stabilized. As seen in Table 2, there was an increase in the pH at equilibrium. Titanates generally behave as weak acids and are hydrolyzed in solutions where protons from the solution are adsorbed and sodium ions are released, thus augmenting the pH of the solution. Higher pH values were noticed especially at lower concentrations. There is the possibility of precipitation which explains the high adsorption percentages at these concentrations. The other pH values were found to be 7 or even lower and the influence of precipitation in these cases could be minimal.

The pH at which sodium iron titanates exhibit maximum Ni adsorption was determined by studying the adsorption percentage as a function of pH. The pH range 2–8 was chosen for the experiment and 0.05 M HCl and 0.05 M NaOH was used to stabilize the pH to the required range. The maximum pH of 8 and initial Ni concentration of 10 mg/l were selected to minimize the influence of precipitation affecting the results. At 20 mg/l concentration, hydroxide ions precipitate Ni at pH > 8 [6]. The adsorption percentage, as a function of equilibrium pH (pH_e), is presented in Fig. 7, from which increase of sorption from pH 2 to 8 can be observed. In case of $SFeTi_9$, sorption was 9% at pH 2, following with a steep rise to 93% at pH 4 and the maximum adsorption of 99% was attained at pH 5. In the case of CFe_2Ti_6, no adsorption occurred at pH 2 but adsorption gently increased at pH 4 (5%) and reached maximum (63%) at pH 8. On the other hand, CFeTi exhibited no adsorption of Ni at pH ≤ 4. Slight adsorption was then observed at pH 5 (7%) with a gentle increase to maximum adsorption (45%) at pH 8. The optimum pH for all three sodium iron titanates proved to be above pH 5 as a clear adsorption trend was observed which indicates that there was little or no adsorption at low pH and high adsorption at high pH. This is understandable because titanates are known to behave as weak acid ion exchangers. In acidic pH, the exchangers will preferably adsorb and retain H^+ from the surrounding medium and thus blocking the exchange sites for nickel ions.

The adsorption isotherm and thus the apparent ion exchange capacity were determined. The adsorption isotherms considered in this study are the Langmuir and Freundlich models. The Langmuir plot of C_e/Q_e against C_e (Fig. 8) for all the initial concentration studied is found to be linear with a correlation coefficient (R^2) of 0.9998 for $SFeTi_9$, 0.9938 for CFe_2Ti_7 and 0.8007 for CFeTi. The good linearity obtained for $SFeTi_9$ and CFe_2Ti_6 indicates the applicability of Langmuir adsorption isotherm to describe these exchangers/Ni systems. In general, the exchangers/Ni systems show a better fitting with the Langmuir than the Freundlich isotherm. The agreement of the experimental data with the Langmuir isotherm implies that nickel is adsorbed as a single layer on the surfaces of the

Table 2
The equilibrium pH values of sodium iron titanates in Ni solution at 10–200 mg/l initial concentration at initial pH of 4.86–5.47

Initial concentration (mg/l)	$SFeTi_9$		CFe_2Ti_6		CFeTi	
	pH_e	%Sorption	pH_e	%Sorption	pH_e	% Sorption
10	6.58	98.66	9.76	99.33	9.05	99.33
30	7.60	99.99	9.13	99.99	8.47	61.27
60	7.77	99.82	7.79	97.06	7.20	34.4
100	6.10	96.7	6.95	63.98	7.05	12.88
150	6.03	65.75	5.50	28.29	6.37	6.17
200	6.13	49.79	5.75	20.36	6.20	9.31

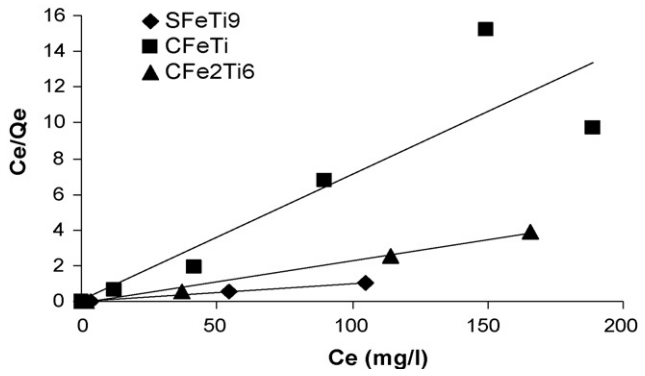

Fig. 8. Linear plot of Langmuir adsorption isotherm of sodium iron titanate/Ni system at room temperature, constant batch factor of 1000 ml/g and initial concentrations of 10–200 mg/l.

adsorbents [36]. The correlation coefficients for the Freundlich values were < 0.5 and thus their adsorption capacities were not calculated. According to the Langmuir isotherms, maximum adsorption capacities were as follows: 104 mg/g for $SFeTi_9$ and 43 mg/g for CFe_2Ti_6. These values are in correlation with the adsorption percentages, where $SFeTi_9$ exhibits the best ion exchange performance. The adsorption capacity for CFeTi was not calculated since the linearity was poor.

To study the selectivity of the ion exchangers for Ni, K_d of Ni was investigated as a function of different K concentrations in the range of 200–1500 mg/l (Fig. 9). The K_d of Ni for CFeTi and CFe_2Ti_6 was observed to be very low through out the entire K concentration range. $SFeTi_9$ on the other hand had high K_d values. The K_d values increases with initial K concentration until the maximum value at 800 mg/l, after which the K_d value decreases again. Due to the high K_d values it can be concluded that Ni has a higher preference of being removed in solutions containing K ions using $SFeTi_9$ ion exchanger.

A pattern that was observed with the ion exchange properties of the sodium iron titanates is as follows: $SFeTi_9$ attains equilibrium in a shorter time (3 h), exhibits higher selectivity of Ni in solutions containing K and has higher adsorption capacity than CFeTi and CFe_2Ti_6. The reason for the superior ion exchange properties of $SFeTi_9$ as compared to CFeTi and CFe_2Ti_6 can be explained based on the shape of the framework structure. $SFeTi_9$ is proposed to be a layered titanate, i.e. isostructural to the parent sodium nonatitanate. Like all layered titanates the exchangeable sodium ions are located between the layers which are easily accessible to incoming Ni^{2+} ions. On the contrary, CFeTi and CFe_2Ti_6 have one-dimensional tunnel structures with the exchangeable sodium ions enclosed within the tunnels [27,37]. Papp et al. [9] reported that titanates with tunnel structures have lower ion exchange properties because exchangeable sodium ions are boxed in by the titanate units in the structure and therefore not easily accessible for exchange.

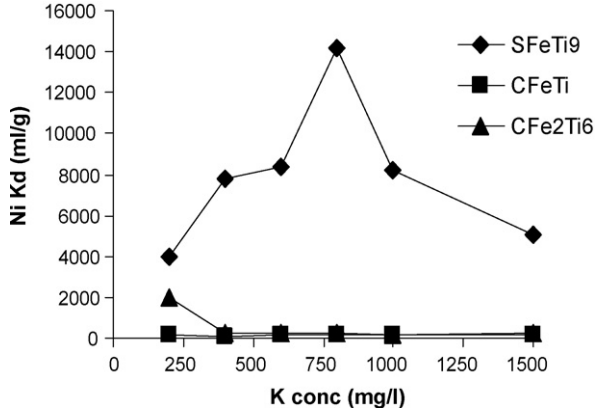

Fig. 9. Plot of K_d versus K concentrations ranging from 200 to 1500 mg/l and constant initial Ni concentration of 100 mg/l to indicate the selectivity of sodium iron titanates for Ni over K.

Also, the ion exchange properties are greatly influenced by the method of preparation of a material. It should be kept in mind that $SFeTi_9$ was prepared by sol–gel method while CFeTi and CFe_2Ti_6 were synthesized via the conventional solid-state procedures. The materials prepared by conventional solid-state method showed poor uptake behavior of Ni. According to Möller et al. [33], the ion exchange properties of ion exchangers prepared by conventional solid-state synthesis are greatly reduced. The preparative method, which involves heating the precursor materials at high temperatures, also involves the removal of structural water and hydroxyl groups resulting in a decrease in ion exchange capacity.

Another possible reason for the high performance of $SFeTi_9$ is the low crystallinity of the compound. It is generally known that ion exchange capacity decreases with increasing crystallinity. For all the titanates synthesized, CFeTi and CFe_2Ti_6 are crystalline whereas $SFeTi_9$ is a semi/poorly crystalline compound. The general degree of crystallinity was observed from the peak widths and the overall intensity gains of the measured XRD patterns, which were compared to diffraction patterns found in the literature [35].

4. Conclusion

A new iron-doped sodium nonatitanate was synthesized in conjunction with existing sodium iron titanates: $NaFeTiO_4$ and $Na_2Fe_2Ti_6O_{16}$. The ion exchange characterization in the removal of heavy metal with Ni as a case study was investigated for the sodium iron titanates. Due to the difference in structure and method of preparation the sodium iron titanates exhibited differences in the ion exchange behavior. Iron-doped sodium nonatitanate exhibited the best ion exchange performance when compared to the other two sodium iron titanates. It is observed to have attained equilibrium in a relatively short time (3 h) with 99.9% of Ni being removed, as oppose to 24 h for $NaFeTiO_4$ and $Na_2Fe_2Ti_6O_{16}$. The distribution coefficient of Ni is appreciatively high even in high potassium concentrations (1500 mg/l). The apparent ion exchange capacity is calculated according to the Langmuir fit to be 104 mg/g and only 43 mg/g for $Na_2Fe_2Ti_6O_{16}$ under the given experimental conditions. The optimal pH in the exchange of Ni is in slightly acidic and basic media, i.e. pH > 5. Since iron-doped sodium nonatitanate is particularly selective for Ni in K solutions, it is a suitable ion exchanger in removing trace Ni in the presence of bulk cations such as potassium.

Acknowledgements

The authors are grateful to the city of Mikkeli and the Finnish Funding Agency for Technology and Innovation (TEKES) for providing the necessary funds to carryout the research successfully.

References

[1] S. Rengaraj, C.K. Joo, Y. Kim, J. Yi, Kinetics of removal of chromium from water and electronic process wastewater by ion exchange resins: 1200H, 1500H and IRN9H, J. Hazard. Mater. B 102 (2003) 257–275.
[2] K.S. Hui, C.Y.H. Chao, S.C. Kot, Removal of mixed metal ions in wastewater by zeolite 4A and residual products from recycled coal fly ash, J. Hazard. Mater. B 127 (2005) 89–101.
[3] F.G. Helfferich, Ion Exchange, Dover Publications, Inc., New York, 1995.
[4] C.E. Harland, Ion Exchange Theory and Practice, 2nd ed., Royal Society of Chemistry, Cambridge, 1994.
[5] M.M. Abou Mesalam, I.M. El-Naggar, Diffusion mechanism of Cs^{+}, Zn^{2+} and Eu^{3+} ions in the particles of zirconium titanate ion exchanger using radioactive tracers, Colloids Surf. A 215 (2003) 205–211.
[6] H. Leinonen, J. Lehto, A. Mäkelä, Purification of nickel and zinc from waste waters of metal-plating plants by ion exchange, React. Polym. 23 (1994) 221–228.
[7] V. de, A. Cardoso, A.G. de Souza, P.C. Patricia, L.M. Nunes, The ionic exchange process of cobalt, nickel and copper(II) in alkaline and acid-layered titanates, Colloids Surf. A 248 (2004) 145–149.
[8] L.N. Nunes, A. Gouveia de Souza, R. Fernandes de Farias, Synthesis of new compounds involving layered titanates and niobates with copper(II), J. Alloys Compd. 319 (2001) 94–99.
[9] S. Papp, L. Korosi, V. Meynen, P. Cool, E.F. Vansant, I. Dekany, The influence of temperature on the structural behavior of sodium tri-and hexatitanates and their protonated forms, J. Solid State Chem. 178 (2005) 1614–1619.
[10] M.M. Abou-Mesalam, Applications of inorganic ion exchangers. II. Adsorption of some heavy metal ions from their aqueous waste solution using synthetic iron(III) titanate, Adsorption 10 (2004) 87–92.
[11] L.M. Nunes, V. de, A. Cardoso, C. Airoldi, Layered titanates in alkaline, acidic and intercalated with 1,8-octyldiamine forms as ion-exchangers with divalent cobalt, nickel and copper cations, Mater. Res. Bull. 41 (2006) 1089–1096.
[12] A. Nilchi, B. Maalek, A. Khanchi, M.G. Maragheh, A. Bagheri, Cerium(IV) molybdate cation exchanger: synthesis, properties and ion separation capabilities, Radiat. Phys. Chem. 75 (2006) 301–308.
[13] A.P. Gupta, G.L. Verma, S. Ikram, Studies on a new heteropolyacid-based inorganic ion exchanger; zirconium(IV) selenomolybdate, React. Funct. Polym. 43 (2000) 33–41.
[14] S.A. Nabi, M. Naushad, Inamuddin, Synthesis and characterization of a new inorganic cation-exchanger-Zr(IV) tungstomolybdate: analytical applications for metal content determination in real sample and synthetic mixture, J. Hazard. Mater. 142 (2007) 404–411.
[15] S.A. Nabi, A.M. Khan, Synthesis, ion exchange properties and analytical applications of stannic silicomolybdate: effect of temperature on distribution coefficients of metal ions, React. Funct. Polym. 66 (2006) 495–508.
[16] V.S. Bergamaschi, F.M.S. Carvalho, C. Rodrigues, D.B. Fernandes, Preparation and evaluation of zirconia micropheres as inorganic exchangers in adsorption of copper and nickel ions and as catalyst in hydrogen production from bioethanol, Chem. Eng. J. 112 (2005) 153–158.
[17] Y.S. Dzyazko, L.M. Rozhdestvenska, A.V. Palchik, F. Lapicque, Ion exchange properties and mobility of Cu^{2+} ions in zirconium hydrophosphate ion exchangers, Sep. Purif. Technol. 45 (2005) 141–146.
[18] S.A. Nabi, M. Naushad, Studies of cation-exchange thermodynamics for alkaline earths and transition metal ions on a new crystalline cation-exchanger aluminum tungstate: effect of the surfactant's concentration on distribution coefficients of metal ions, Colloids Surf. A 293 (2007) 175–184.
[19] I.M. El-Naggar, E.A. Mowafy, Y.f. El-Aryan, M.G. Abd El-Wahed, Sorption mechanism for Cs^{+}, Co^{2+} and Eu^{3+} on amorphous zirconium silicate as cation exchanger, Solid State Ion. 178 (2007) 741–747.
[20] S.A. Nabi, A.H. Shalla, A.M. Khan, S.A. Ganie, Synthesis, characterization and analytical applications of titanium(IV) molybdosilicate: a cation ion-exchanger, Colloids Surf. A 302 (2007) 241–250.
[21] J.H. Choi, S.D. Kim, S.H. Noh, S.J. Oh, W.J. Kim, Adsorption behaviours of nano-sized ETS-10 and Al-substituted ETAS-10 in removing heavy metal ions, Pb^{2+} and Cd^{2+}, Micropor. Mesopor. Mater. 87 (2007) 163–169.
[22] L. Lv, K. Wang, X.S. Zhao, Effect of operating conditions on the removal of Pb^{2+} by microporous titanosilicate ETS-10 in a fixed bed column, J. Colloid Interface Sci. 305 (2007) 218–225.
[23] S.P. Mishra, S.S. Dubey, D. Tiwari, Inorganic particulates in removal of heavy metal toxic ions IX. Rapid and efficient removal of Hg(II) by hydrous manganese and tin oxides, J. Colloid Interface Sci. 279 (2004) 61–67.
[24] S. Mishra, Vijaya, Inorganic particulates in removal of heavy metal toxic ions. Part X. Rapid and efficient removal of Hg(II) ions from aqueous solutions by hydrous ferric and hydrous tungsten oxides, J. Colloid Interface Sci. 296 (2006) 383–388.
[25] R.R. Bel, G.C. Saunders, Cadmium adsorption on hydrous aluminium(III) oxide: effect of adsorbed polyelectrolyte, Appl. Geochem. 20 (2005) 529–536.
[26] M.M. Abou-Mesalam, Sorption kinetics of copper, zinc, cadmium and nickel ions on synthesized silico-antimonate ion exchanger, Colloids Surf. A 225 (2003) 85–94.
[27] J. Akimoto, Y. Takahashi, N. Kijima, Y. Gotoh, Synthesis and structural analysis of a new sodium iron titanate $Na_{2+x}Fe_xTi_{4-x}O_9$ with $x = 0.6$, Solid State Ion. 172 (2004) 495–497.
[28] A. Kuhn, F. Garcia-Alvarado, E. Moran, M.A. Alario-Franco, U. Amador, Structural effects of sodium extraction on $Na_xFe_xTi_{2-x}O_4$ single crystals, Solid State Ion. 86–88 (1996) 811–818.
[29] P. Ondrus, R. Skala, K. Bowen, Bede ZDS Search/Match for Windows, vol. 4.51, Bede Scientific Instruments Ltd., Durham, United Kingdom, 2000.
[30] ICDD International Centre for Diffraction Data, Powder Diffraction File Sets 1–51, Newton Square, Pennsylvania, 2001.
[31] A. Clearfield, J. Lehto, Preparation, structure, and ion exchange properties of $Na_4Ti_9O_{20}\cdot xH_2O$, J. Solid State Chem. 73 (1988) 98–106.
[32] A.-L. Sauvet, S. Baliteau, C. Lopez, P. Fabry, Synthesis and characterization of sodium titanates $Na_2Ti_3O_7$ and $Na_2Ti_6O_{13}$, J. Solid State Chem. 177 (2004) 4508–4515.
[33] T. Möller, A. Clearfield, R. Harjula, Preparation of hydrous mixed metal oxides of Sb, Nb, Si, Ti and W with a pyrochlore structure and exchange of radioactive cesium and strontium ions into the materials, Micropor. Mesopor. Mater. 54 (2002) 187–199.
[34] J. Lehto, R. Harjula, Selective separation of radionuclides from nuclear waste solutions with inorganic ion exchangers, Radiochim. Acta 86 (1999) 65.
[35] P. Sylvester, T. Möller, T.W. Adams, A. Cisar, Improved separation methods for the recovery of ^{82}Sr from irradiated targets, Appl. Radiat. Isot. 64 (2006) 422–430.
[36] S.-Y. Kang, J.-U. Lee, S.-H. Moon, K.-Y. Kim, Competitive adsorption characteristics of Co^{2+}, Ni^{2+}, Cr^{3+} by IRN-77 cation exchange resin in synthesized waste water, Chemosphere 56 (2004) 141–147.
[37] Y. Michiue, Phase relations in $Na_xCr_xTi_{8-x}O_{16}$ at 1350 °C and crystal structure of hollandite-like $Na_2Cr_2Ti_6O_{16}$, J. Solid State Chem. 179 (2006) 2578–2583.